COMPARISON OF GPS-BASED ORBIT DETERMINATION STRATEGIES

E. Gill, O. Montenbruck

Deutsches Zentrum für Luft- und Raumfahrt (DLR) e.V., German Space Operations Center, 82234 Wessling, Germany, eberhard.gill@dlr

ABSTRACT

Orbit determination strategies for the on-ground trajectory reconstruction of Low Earth Orbit satellites are compared. The analyzed strategies involve different GPS measurement types comprising navigation solution, single or dual-frequency pseudorange, as well as carrier phase measurements. Furthermore, different processing techniques such as kinematic or reduced-dynamic processing are addressed. Two sample sets of GPS BlackJack measurements are employed, that were obtained in the framework of the CHAMP mission. It is shown that the resulting position accuracy ranges, depending on the adopted strategy, from 10 m to better than 10 cm.

1. INTRODUCTION

Spaceborne GPS receivers have advanced over the past years to the primary tracking sensors for Low Earth Orbit (LEO) satellites. Onboard the spacecraft, GPS-derived orbit knowledge may greatly enhance the mission capabilities e.g. through autonomous navigation functions. At the same time, GPS tracking has a severe impact on the strategies for the on-ground reconstruction of the spacecraft orbit.

Single frequency L1 GPS receivers may vary in the delivered data types which range from position fixes to raw data. The latter may comprise C/A- and P-code pseudoranges as well as carrier phase measurements. In addition, geodetic-type receivers may deliver L2 P-code and L2 carrier phase which, in the end, opens up a variety of approaches to orbit determination.

Finally, different data sets may be treated in a kinematic, reduced-dynamic, or fully dynamic way, depending on the amount of orbit knowledge included in the processing. The paper provides a description of the involved precise orbit determination (POD) algorithms and evaluates the suite of POD strategies with emphasis to a reduced-dynamic treatment.

2. THE GPS RECEIVER ON CHAMP

To evaluate different orbit determination strategies, GPS data from the Challenging Minisatellite Payload (CHAMP) mission are employed. CHAMP is a German small satellite for geoscientific and atmospheric research [1] which was launched on 15 July 2000 into a near-circular, near-polar, low Earth orbit.

The spacecraft carries a BlackJack GPS receiver, developed for NASA by the Jet Propulsion Laboratory (JPL). BlackJack is a geodetic-type dual-frequency receiver with a total of 48 channels which are connected to four antennas using a matrix switch [2]. The individual channels can be allocated to track C/A-, P1- and P2-code for up to 16 satellites, with a typical limit of 10 satellites employed on CHAMP.

3. ORBIT DETERMINATION STRATEGIES

3.1 GPS Data Types and Linear Combinations

Besides the navigation solutions with its three position and velocity components, nine data types are provided in the raw CHAMP observation files. These comprise the C/A-code (C1), two P-code measurements (P1 and P2) as well as carrier phase measurements (LA, L1, L2) and signal-to-noise-ratios (SNR) for each of the associated tracking channels (SA, S1, S2). The BlackJack receiver provides two independent carrier phase observables on L1: LA generated by the C/A-code and L1 by the P1-code tracking channels.

The characteristics of the raw measurement types may be described by the following measurement model equations

$$\begin{aligned}
\rho_{\mathrm{CA}} &= \rho + c\Delta\delta t + b_{\mathrm{CA}} + I + M_{\mathrm{CA}} + \varepsilon_{\mathrm{CA}} \\
\rho_{\mathrm{P1}} &= \rho + c\Delta\delta t + b_{\mathrm{P1}} + I + M_{\mathrm{P1}} + \varepsilon_{\mathrm{P1}} \\
\rho_{\mathrm{P2}} &= \rho + c\Delta\delta t + b_{\mathrm{P2}} + I f_1^2/f_2^2 + M_{\mathrm{P2}} + \varepsilon_{\mathrm{P2}} \\
\rho_{\mathrm{LA}} &= \rho + c\Delta\delta t - \lambda_1 N_{\mathrm{LA}} + b_{\mathrm{LA}} - I + M_{\mathrm{LA}} + \varepsilon_{\mathrm{LA}} \\
\rho_{\mathrm{L1}} &= \rho + c\Delta\delta t - \lambda_1 N_{\mathrm{L1}} + b_{\mathrm{L1}} - I + M_{\mathrm{L1}} + \varepsilon_{\mathrm{L1}} \\
\rho_{\mathrm{L2}} &= \rho + c\Delta\delta t - \lambda_2 N_{\mathrm{L2}} + b_{\mathrm{L2}} - I f_1^2/f_2^2 + M_{\mathrm{L2}} + \varepsilon_{\mathrm{L2}}
\end{aligned} \tag{1}$$

where ρ denotes the geometric distance between the phase centers of the transmitting and receiving GPS antennas. The clock error difference of the GPS satellite and the GPS receiver is denoted by $c\Delta\delta t$ and I denotes the ionospheric path delay for the L1 frequency. Integer multiples of the respective wavelength (e.g. $\lambda_1 N_{\mathrm{LA}}$) denote the carrier phase ambiguities and b is an additional inter-channel difference and line bias. Finally, each measurement type is affected by a specific multipath (M) and exhibits a specific random noise (ε).

For dual frequency receivers, ionosphere-free pseudo-range measurements ρ_{P12} are obtained from

$$\rho_{P12}=\frac{f_1^2}{f_1^2-f_2^2}\rho_{P1}-\frac{f_2^2}{f_1^2-f_2^2}\rho_{P2}\approx 2.546\rho_{P1}-1.546\rho_{P2} \quad (2)$$

with a noise level about three times larger than for single frequency measurements [3]. A corresponding relation holds for ionosphere-free carrier phase measurements ρ_{L12}.

In single frequency GPS positioning the problem of ionospheric path delays can also be overcome by using a specific linear combination of code and carrier phase measurements. The so-called GRAPHIC (Group and Phase Ionospheric Calibration,[4]) data type

$$\begin{aligned}\rho^* &= (\rho_{CA}+\rho_{L1})/2 \\ &= \rho + c\Delta\delta t - \lambda_1 N_{L1}/2 + b^* + M^* + (\varepsilon_{CA}+\varepsilon_{L1})/2\end{aligned} \quad (3)$$

exhibits a noise level of about half the C/A code noise. However, the measurement bias $\lambda_1 N_{L1}/2$ is introduced which differs for each channel and inhibits the direct use of GRAPHIC data for single point positioning.

3.2 Dynamic Orbit Determination Strategies

Instead of a purely kinematic positioning from raw GPS measurements, the additional use of orbit knowledge from the equations of motion may substantially improve the orbit determination accuracy. The dynamic model adopted in the present analysis comprises the aspherical gravitational field of the Earth (100x100 subset of the model GGM01S), atmospheric drag (Jacchia 1971 model), third-body forces from the sun and moon, solar radiation pressure, as well as solid Earth tide, ocean and pole tides [5]. To account for deficiencies in the deterministic models, empirical accelerations in the radial, tangential, and normal (RTN) directions are considered. Independent sets of empirical accelerations are estimated for consecutive intervals of typically 600s. Thus, the dynamic state $\boldsymbol{Y}$ is given by

$$\boldsymbol{Y}=\left(\boldsymbol{y}_0, C_R, C_D, a_R^i, a_T^i, a_N^i\right) \quad (4)$$

where $\boldsymbol{y}_0$ denotes the epoch state vector, C_R the solar radiation pressure coefficient, C_D the drag coefficient and $(a_R, a_T, a_N)^i$ the i^{th} vector of empirical accelerations. in the considered data arc.

The investigated orbit determination strategies are essentially based on the global adjustment of dynamic parameters, receiver clock offsets, and, when carrier phases are involved, carrier phase biases. Depending on the GPS receiver type, four zero-difference measurement types are applied: C/A code, ionosphere-free pseudorange, GRAPHIC, and ionosphere-free carrier phase.

The most complex orbit determination strategy is based on carrier phase measurements, where measurement biases have to be solved for. Prior to the global parameter adjustment, a careful data screening and editing is required. Furthermore, a priori clock offsets are determined from the pseudoranges. In addition, the start and stop times of continuous carrier phase arcs without cycle slips have to be established. These tasks require precise a priori information of the user satellite orbit, which may, e.g. be derived from a reduced-dynamic post-processing of single point positioning solutions in a previous step.

When processing GRAPHIC or dual-frequency carrier phase measurements, the dynamic state $\boldsymbol{Y}$ may be supplemented by the vector $\boldsymbol{B}$ of measurement biases according to $\boldsymbol{X} = (\boldsymbol{Y}, \boldsymbol{B})$. Further unknowns in the orbit determination comprise the receiver clock offsets per epoch δt_i which may be combined into a vector $\boldsymbol{T}$

$$\boldsymbol{T}=\left(c\delta t_1,\ldots,c\delta t_J\right). \quad (5)$$

Thus, the global adjustment of the unknowns $\boldsymbol{Y}$, $\boldsymbol{B}$, and $\boldsymbol{T}$ is achieved through the solution of the normal equations which may be written in block structure as

$$\begin{pmatrix}\boldsymbol{N}_{TT} & \boldsymbol{N}_{TX}\\ \boldsymbol{N}_{XT} & \boldsymbol{N}_{XX}\end{pmatrix}\begin{pmatrix}\Delta\boldsymbol{T}\\ \Delta\boldsymbol{X}\end{pmatrix}=\begin{pmatrix}\boldsymbol{n}_T\\ \boldsymbol{n}_X\end{pmatrix}. \quad (6)$$

However, due to the large number of unknowns a direct solution of the full normal equations is replaced by a block elimination based on the fact, that the largest matrix $\boldsymbol{N}_{TT}$ is diagonal. Corrections of the a priori parameters $\boldsymbol{X}_{ap}$ are then obtained from the expression

$$\Delta\boldsymbol{X}=\left(\boldsymbol{N}_{XX}-\boldsymbol{N}_{XT}\boldsymbol{N}_{TT}^{-1}\boldsymbol{N}_{TX}\right)^{-1}\left(\boldsymbol{n}_X-\boldsymbol{N}_{XT}\boldsymbol{N}_{TT}^{-1}\boldsymbol{n}_T\right) \quad (7)$$

which is employed to derive the receiver clock corrections

$$\Delta\boldsymbol{T}=\boldsymbol{N}_{TT}^{-1}\left(\boldsymbol{n}_T-\boldsymbol{N}_{TX}\Delta\boldsymbol{X}\right). \quad (8)$$

Typically for a 24 hour data arc, about 420 passes of continuous carrier phase data are identified and, based on 10 min. segments, a total of about 430 empirical acceleration components are considered. In addition, based on a measurement sampling interval of 30 s, a total of 2880 receiver clock offsets are estimated.

When processing only pseudoranges (C/A-code resp. ionosphere-free pseudorange), similar but simplified expressions may easily be derived, since no bias parameters are present in this case.

4. EVALUATION OF POD STRATEGIES

4.1 Selected GPS Data Sets

Two sample sets of CHAMP GPS data have been selected. The first data set covers the period of 2001/05/20-30 (day of year (DOY) 140-150), which has been adopted by the International GPS Service (IGS) LEO pilot project groups [6]. Data from this period do not provide the high measurement accuracy of later periods. On the other hand, the dynamic environment in this period is benign due to the modest solar and geomagnetic activity. Furthermore, at a mean altitude of 432 km the CHAMP satellite is less susceptible to atmospheric drag and small scale irregularities in the Earth's gravity field than in later parts of the mission.

The second data set covers the period of 2003/10/22-/11/01 (DOY 295-305). In contrast to the first data set, it provides data of generally high quality, which have been recorded during a massive solar storm. Here, the daily solar flux values $F_{10.7}$ rose from a typical level of 100 up to 300 while the 3-hourly K_p index, reflecting the geomagnetic activity, increased from typical values of 3-5 up to 9. Also the CHAMP mean altitude of 391 km is more than 40 km below the altitude in the first data set. Hence, the second period represents a major challenge for the dynamic modelling of the spacecraft motion. As consequence of the solar storm maximum on 2003/10/26, the ionosphere was heavily perturbed with a time lag of about 3 days, where the typical maximum total electron content (TEC) increased from 90 to 230 TEC units on 2003/10/29. Therefore, ionospheric perturbations on the raw GPS data are much more pronounced for the second than for the first data arc.

The raw GPS measurements are provided at a standard data interval of 10 s. Based on nine active channels, a total of 200,000 pseudorange (C1, P1 and P2) and 200,000 carrier phase (LA, L1 and L2) data are typically provided per day. The noise of the carrier-smoothed pseudoranges varies between a minimum of 5 cm at high elevations and 0.5 m (C1) or 1.0 m (P1, P2) at 10 deg elevation. Aside from data noise, the code measurements obtained in the aft-looking hemisphere suffer from systematic of up to several meters that are further discussed in [7]. The noise of the carrier phase data appears to vary throughout the CHAMP mission due to different software versions running within the BlackJack receiver. The L1 carrier phase noise at high elevations was about 0.15 mm in May 2001 and 0.6 mm in July 2002. At both epochs, the noise at 10 deg elevation was about 2.8 mm [7].

In addition to the raw GPS data, navigation solutions from the BlackJack receiver are provided. In the first arc, these navigation solutions exhibit a typical mean position error of 20 m 3D r.m.s. which reduces to 13 m 3D r.m.s. in the second arc. This improvement may be attributed to a sequence of receiver software uploads which were performed between these periods. It is noted, however, that a particular day (2003/295) exhibited position residuals of about 90 m 3D r.m.s. Such outliers highlight problems which may be encountered when using unfiltered GPS navigation solutions onboard a spacecraft. A summary of the main characteristics of the selected data arcs is provided in Table 1.

Table 1. Characteristics of CHAMP selected data arcs

Data Arc	Year/DOY	Mean alt. [km]	Maximum solar flux	Max. TEC [TECU]
#1	2001/140-150	432	180	94
#2	2003/295-305	391	300	229

4.2 CHAMP Reference Orbits and IGS Products

The quality of the computed CHAMP trajectories has been assessed based on daily reference orbit files. For the first arc in 2001, the reference orbits were provided by the Institute of Astronomical and Physical Geodesy (iapg) of the Technical University of Munich. The Rapid Science Orbits (RSO) of the CHAMP Information System and Data Center (ISDC) [8] were applied as reference orbits for the second arc in 2003. For both arcs, the quality of the CHAMP reference positions is expected to be better than 5 cm 3D r.m.s.

The quality of GPS-based orbit determination depends crucially on the applied GPS orbit and clock solutions. Since the analysis is focused on off-line orbit determination strategies, only IGS final orbit and clock products have been employed. These products are provided with a latency of about 13 days and provide GPS orbits with a sampling of 15 mins, while the clock products are sampled at 5 mins intervals.

4.3 A Priori Orbits for a Robust Data Editing

Any orbit determination using GPS pseudorange and carrier phase data depends crucially on the ability to remove invalid or degraded measurements from the estimation process and identify carrier phase cycle slips. Since a precise user orbit is a prerequisite for a successful data editing, an iterative step-wise approach of data editing and orbit adjustment is advised.

In order to generate an adequate a priori orbit for the final orbit adjustment, a two step approach has been implemented. Here, the first step consists of a classical kinematic single point positioning (SPP) based on single- or double-frequency pseudoranges while the second step involves a reduced-dynamic filtering of the kinematic SPP positions.

The SPP applies a series of basic edit criteria comprising thresholds for the SNR, the elevation of the GPS satellite in the spacecraft antenna system, as well as the standard deviation of the pseudorange residuals.

In addition, the difference of code and carrier delta measurements, obtained from a differencing of measurements at subsequent epochs, allows the identification of outliers. Finally, only epochs are taken into account for which the number of observed satellites exceeds a certain limit and where the Position Dilution of Precision (PDOP) is below a specified threshold. In case of the two selected data arcs, the SPP editing removes about 10% of the epochs for arc #1 and 3% for arc #2.

The position accuracy for the SPP solutions is summarized in Table 2. Here, the position differences of the SPP and reference orbits have been mapped onto the orbit frame components in radial (*R*), tangential (*T*), and normal (*N*) directions. As can be seen, single frequency SPP solutions yield position errors of 8-10 m, depending on the data noise, the observation geometry and, predominantly, the ionospheric conditions. The average of the daily mean radial error is 4.9 m and 6.4 m for arc#1 and #2, respectively and dominates the tangential and normal components. These radial errors stem from ionospheric perturbations [9] and days with highest TEC values yield the worst position solutions. In contrast, a dual frequency SPP strategy is account for ionospheric delays and achieve a position accuracy of 2-4 m 3D r.m.s. depending on the data quality. Still, the radial error component is dominant which is mainly caused by the higher Dilution of Precision (DOP) values in radial direction.

Table 2. Single Point Positioning kinematic position accuracy in the orbital frame (R, T, N)

Arc	Average r.m.s. [m]			
	Radial	Tangential	Normal	Total
Single frequency				
#1	7.39	2.01	1.36	7.78
#2	10.25	1.78	1.33	10.49
Dual frequency				
#1	3.04	1.71	1.06	3.68
#2	1.92	0.76	0.61	2.15

The resulting SPP solution still is not adequate for data editing purposes, since it neither achieves the required accuracy nor is it, due to its kinematic nature, continuous. Both drawbacks may conveniently be overcome by a reduced-dynamic post-processing of SPP position solutions. To this end, a dynamic modelling has been applied which accounts for empirical acceleration batches of 10 mins duration with appropriate a priori sigmas (10, 25, 50 nm/s^2 for the *R*, *T*, *N* acceleration components in this specific case). This approach allows both to introduce orbital knowledge to the system as well as to compensate for remaining modelling deficiencies.

As can be seen in Table 3, the reduced-dynamic post-processing of SPP solutions achieves a position accuracy of 0.7-1.0 m (3D r.m.s.) with single and 0.2-0.3 m (3D r.m.s.) with double frequency SPP solutions. Although all orbital frame components gain in accuracy from the dynamic treatment, the major benefit stems from the reduction of the radial position error inherent to the kinematic solution. The accuracy of the post-processed solution is finally limited by errors in the along-track position components. The resulting CHAMP orbit achieves a rough order of magnitude improvement in accuracy over the SPP solutions and provides a continuous trajectory. It thus serves as a suitable a priori orbit for the data editing within the global orbit adjustment from raw GPS data.

Table 3. Post-processing of Single Point Positioning solutions in a reduced-dynamic approach

Arc	Average r.m.s. [m]			
	Radial	Tangential	Normal	Total
Single frequency				
#1	0.36	0.90	0.15	0.98
#2	0.25	0.59	0.18	0.67
Dual frequency				
#1	0.07	0.20	0.08	0.22
#2	0.11	0.28	0.07	0.31

4.4 Dynamic Orbit Determination Results

A fully dynamic orbit determination without the adjustment of empirical accelerations provides, at least from a software point-of-view, the simplest orbit determination strategy. In this case, the achievable accuracy depends crucially on the data arc length. A convenient length for an automated processing scheme is a 24 hr arc, which is applied throughout the analysis. Upon processing of GPS navigation solutions, an average position error of 3.4 m is achieved for the first and 33.1 m (3D r.m.s.) for the second arc. Thus, this approach may, in general, improve the accuracy of unfiltered navigation solution by a factor of up to 5. However, a severe degradation has been observed for days with high dynamic perturbations resulting in position errors as high as 60 m (3D r.m.s.) which causes the high average value of 33.1 m for the second arc. As consequence, a dynamic processing of one day arcs is ruled out for an automated processing and only reduced-dynamic strategies have been considered in the sequel.

Upon applying navigation solutions in a reduced-dynamic orbit determination, the inherent noise of the measurements is greatly absorbed in the data residuals. Moreover, any dynamic mismodelling is absorbed in the considered empirical accelerations. Thus, this strategy substantially improves the pure navigation solution accuracy and yields position errors of less than 2 m as shown in Table 4.

Although the error budget is dominated by the along-track component, the harsh dynamic perturbations during data arc #2 are effectively absorbed by the empirical accelerations. Moreover, as consequence of

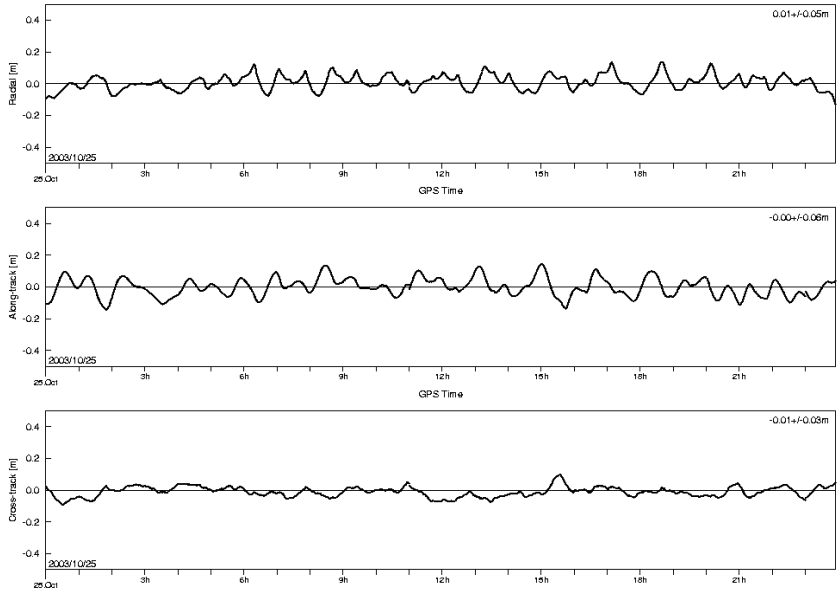

Fig. 1 Position residuals from a reduced-dynamic orbit determination based on dual-frequency pseudorange and carrier phase measurements with respect to a Champ reference orbit

the receiver software update in March 2003 (which increased the number of active channels from 8 to 10) the orbit determination thereafter benefits from significantly improved navigation solutions.

Table 4. Reduced-dynamic orbit determination results from GPS navigation solutions

Arc	Average r.m.s. [m]			
	Radial	Tangential	Normal	Total
#1	0.62	1.80	0.50	1.97
#2	0.47	1.06	0.44	1.25

When GPS pseudoranges are applied in a single global block adjustment based on a precise a priori orbit, a sub-meter position accuracy is achieved (cf. Table 5). Single frequency strategies are still susceptible to the ionospheric errors with position errors of about 0.8 m. In contrast, dual frequency approaches yield position errors of 0.2 m. It is instructive to note that the resulting accuracy figures are roughly comparable to the results from a post-processing of SPP solutions (Table 3).

Table 5. Reduced-dynamic orbit determination results from GPS pseudoranges

Arc	Average r.m.s. [m]			
	Radial	Tangential	Normal	Total
Single frequency				
#1	0.32	0.84	0.16	0.92
#2	0.26	0.63	0.17	0.70
Dual frequency				
#1	0.06	0.15	0.07	0.18
#2	0.11	0.25	0.06	0.28

A detailed list of the daily results from arc #2 reveals that the maximum position errors occur on the two days (2003/303-304) of the ionospheric storm. Ignoring these two days improves the position accuracy from 0.70 m to 0.55 m (single frequency) and from 0.28 m to 0.20 m (dual-frequency). These figures may provide a more realistic estimate of the typical accuracy achievable with this strategy.

The ultimate orbit determination accuracy is expected from the use of low-noise carrier phase measurements. Even for single frequency GPS receivers, the ionosphere may be calibrated based on GRAPHIC data. This enables a position accuracy of about 0.3 m as depicted in Table 6. Focusing on data arc #2 with its better data quality and ignoring the two days of the solar storm, even position errors of 0.19 m are achieved, slightly better than using dual-frequency pseudoranges.

Table 6. Reduced-dynamic orbit determination results from GPS carrier phases

Arc	Average r.m.s. [m]			
	Radial	Tangential	Normal	Total
Single frequency				
#1	0.11	0.28	0.07	0.31
#2	0.09	0.23	0.06	0.25
Dual frequency				
#1	0.05	0.08	0.04	0.10
#2	0.05	0.08	0.04	0.11

Of course, dual frequency carrier phase measurements provide the most accurate input for GPS-based orbit determination. In this analysis, an average r.m.s. value for the 3D position accuracy of 0.1 m has been achieved over 11 one-day data batches. Still, a degradation of the position accuracy by 0.03-0.05 m is observable during heavy ionospheric storms. However, it is noted, that the scatter of the r.m.s. position figures of individual days (0.015 m) is by far the smallest of all investigated strategies, thus proving a very robust method. In terms of accuracy, individual days with a good data coverage

and quality yield position accuracies as good as 0.07 m. Moreover, it is noted that the individual error components in the orbital frame as depicted e.g. in Fig. 1 are largely balanced which indicates an additional strength of this strategy.

To summarize the analyzed strategies, an overview of the achieved orbit determination accuracy depending on the applied data types and the processing strategy is collated in Table 7. Here, the given numbers have been obtained from the average of the total position errors of the two selected data arcs. According to the inherent deficiencies of these arcs, the given numbers are considered to be conservative accuracy estimates.

Table 7. Typical CHAMP position accuracies (3Dr.m.s.)
(PR: pseudorange, CP: carrier phase, SPP: single point positions)

Data Type	Processing Scheme	Accuracy [m]
Navigation solutions	Kinematic	16.5
Navigation solutions	Reduced-dynamic	1.6
Single frequency PR	Kinematic	9.1
Dual frequency PR	Kinematic	2.9
Single frequency SPP	Reduced-dynamic	0.8
Dual frequency SPP	Reduced-dynamic	0.3
Single frequency PR	Reduced-dynamic	0.8
Dual frequency PR	Reduced-dynamic	0.2
Single frequency PR & CP	Reduced-dynamic	0.3
Dual frequency PR & CP	Reduced-dynamic	0.1

5. SUMMARY AND CONCLUSIONS

A suite of strategies has been described and evaluated for the GPS-based orbit determination of LEO satellites. In contrast to high-precision (centimeter-level) orbit reconstructions for geoscientific purposes, the selected strategies are focused on the precise orbit determination for various applications at satellite control centers.

Making use of two data sets from the BlackJack GPS receiver onboard the CHAMP satellite, a wide regime of position accuracies has been found which crucially depends on the applied data types as well on the adopted processing scheme.

The direct use of the receiver's navigation solutions is ruled out due to possible data gaps, a limited position accuracy of about 15 m, and poor velocity estimates. Also, a purely dynamic orbit determination from navigation solutions is not recommended, since the resulting position is susceptible to periods of high dynamic perturbations. However, a reduced-dynamic approach provides an efficient and robust strategy which yields position accuracies better than 2 m.

It has been found that a precise and continuous a priori orbit is crucial for a reliable and robust data editing of raw GPS data. Such orbits were obtained from a reduced-dynamic post-processing of kinematic single point positioning results. This approach yields a position accuracy of about 0.8 m and 0.3 m for single and double frequency scenarios, respectively. For orbit determinations purely based on pseudoranges, position accuracies of 0.8 m and 0.2 m have been found for single and double frequency cases. For receivers delivering pseudoranges and carrier phases, various techniques can be applied to eliminate ionospheric errors. Here, the position error is 0.3 m for single and 0.1 m for double frequency receivers at the expense of a complex and time consuming processing strategy.

Acknowledgement

This study applies BlackJack GPS receiver measurements which have been made available for the CHAMP science team by the GeoForschungsZentrum Potsdam. Precise reference orbits of the CHAMP satellite have kindly been provided by the Institute of Astronomical and Physical Geodesy (iapg) of the Technical University of Munich.

References

1. Reigber C., Bock R., Förste C., Grunwaldt L., Jakowski N., Lühr H., Schwintzer P., Tilgner C., *CHAMP phase B—executive summary*; Scientific technical report STR96/13, GeoForschungsZentrum Potsdam (1996).

2. NASA BlackJack GPS receiver. NASA Tech Briefs NPO-20891, June 2001, http://www.nasatech.com/-Briefs/June01/NPO20891.html (2001).

3. Hofmann-Wellenhof B., Lichtenegger H., Collins J.; *GPS Theory and Practice;* 4th edn. Springer, Berlin Wien New York (1997).

4. Yunck T.P.; *Orbit Determination*; in Parkinson B.W., Spilker J.J. (eds.); *Global Positioning System: Theory and Applications*; AIAA, Washington D.C. (1996).

5. Montenbruck O., Gill E.; *Satellite Orbits - Models, Methods and Applications*; Springer Heidelberg; (2001).

6. Boomkamp H.; *Champ Orbit Test Period*; IGS LEO Mail #14; ftp://cddsia.gsfc.nasa.gov/pub/gps/igsmail/-igsleo.0014 (2001).

7. Montenbruck O., Kroes R.; *In-flight performance analysis of the CHAMP BlackJack GPS Receiver*; GPS Solutions **7**, 74-86 (2003).

8. Announcement of opportunity for CHAMP. CHGFZ-AO-001, Issue 1.0, May 28, 2001, GeoForschungs-Zentrum Potsdam (2001).

9. Montenbruck O., Gill E.; *Ionospheric Correction for GPS Tracking of LEO Satellites*; The Journal of Navigation **55**, 293-304 (2002).